$Cu_2Zn(Sn,Ge)Se_4$ and $Cu_2Zn(Sn,Si)Se_4$ alloys as photovoltaic materials: Structural and electronic properties

Qiang Shu,[1] Ji-Hui Yang,[1] Shiyou Chen,[1,2] Bing Huang,[3] Hongjun Xiang,[1] Xin-Gao Gong,[1] and Su-Huai Wei[3]

[1]*Key Laboratory for Computational Physical Sciences (MOE), State Key Laboratory of Surface Physics, and Department of Physics, Fudan University, Shanghai 200433, China*

[2]*Key Laboratory of Polar Materials and Devices (MOE), East China Normal University, Shanghai 200241, China*

[3]*National Renewable Energy Laboratory, Golden, Colorado 80401, USA*

(Received 16 January 2013; published 27 March 2013)

As alternatives to the mixed-anion $Cu_2ZnSn(S,Se)_4$ alloys, the mixed-cation $Cu_2Zn(Sn,Ge)Se_4$ and $Cu_2Zn(Sn,Si)Se_4$ alloys can also span a band gap range that fits the requirement of the solar cell light absorber. However, material properties of these alloys as functions of alloy composition x are not well known. In this paper, using the first-principles calculations, we study the structural and electronic properties of these alloys. We find that (i) the $Cu_2Zn(Sn,Ge)Se_4$ alloys are highly miscible with low formation enthalpies, while the $Cu_2Zn(Sn,Si)Se_4$ alloys are less miscible; (ii) the band gap of $Cu_2Zn(Sn,Ge)Se_4$ increases almost linearly from 1.0 eV to 1.5 eV as the Ge composition x increases from 0 to 1, whereas the band gap of $Cu_2Zn(Sn,Si)Se_4$ spans a larger range from 1.0 eV to 2.4 eV and shows a slightly larger bowing; and (iii) the calculated band offsets shows that the band gap increase of the alloys with the addition of Ge or Si results primarily from the conduction band upshift, whereas the valence band shift is less than 0.2 eV. Based on these results, we expect that the component-uniform and band-gap-tunable $Cu_2Zn(Sn,Ge)Se_4$ and $Cu_2Zn(Sn,Si)Se_4$ alloys can be synthesized and have an improved photovoltaic efficiency.

DOI: 10.1103/PhysRevB.87.115208 PACS number(s): 61.50.Ah, 71.20.Nr, 71.55.Ht, 72.40.+w

I. INTRODUCTION

Recently, the Cu-based quaternary semiconductors, such as Cu_2ZnSnS_4 and $Cu_2ZnSnSe_4$, have been studied extensively for their potential applications in low-cost, earth-abundant photovoltaic devices.[1–10] At the early stage, the kesterite-structured Cu_2ZnSnS_4 draws intensive attention because its band gap is close to the optimal value ($\sim$1.5 eV) for single-junction solar cell according to the Shockley-Queisser model.[11] Recent experimental reports by different groups, however, show that the solar cells based on $Cu_2ZnSnSe_4$ (with a band gap 1.0 eV)[12,13] or the mixed-anion $Cu_2ZnSn(S,Se)_4$ alloys (with low S composition and band gaps lower than 1.2 eV) have higher efficiency than the Cu_2ZnSnS_4 cells, although the band gaps of the $Cu_2ZnSnSe_4$-based cells deviate from the optimal value.[8,12,14,15] Chen *et al.* compared the defect properties in Cu_2ZnSnS_4 and $Cu_2ZnSnSe_4$ and revealed that the detrimental effects of the deep-level defects are larger in the sulfides than in the selenides, which limits the efficiency of the Cu_2ZnSnS_4 solar cells.[16–20] As a result, although the band gap of the $Cu_2ZnSn(S,Se)_4$ alloys can be tuned to the optimal value, the efficiency improvement is limited. It is thus necessary to explore alternative alloys to $Cu_2ZnSn(S,Se)_4$ that can have band gaps close to 1.4 $\sim$ 1.5 eV and also have benign defect properties, as in the selenide $Cu_2ZnSnSe_4$.

The mixed-cation alloys of $Cu_2ZnSnSe_4$ are possible candidates, for example, mixing Si or Ge on Sn sites, which produces $Cu_2Zn(Sn,Si)Se_4$ or $Cu_2Zn(Sn,Ge)Se_4$ alloys, respectively. Their band gaps can be readily tuned to 1.4 $\sim$ 1.5 eV, and all the component elements are not scarce or toxic. Experimentally, the groups in both Purdue University and IBM Research Center have shown that the $Cu_2Zn(Ge,Sn)(S,Se)_4$ alloys can have good photovoltaic performance, and a power-conversion efficiency as high as 9.1% has been achieved in $Cu_2Zn(Ge,Sn)Se_4$ solar cells (40% Ge-doped $Cu_2ZnSnSe_4$).[21,22] Thus far, however, theoretical understanding of these mixed-cation alloys is still lacking, and many fundamental problems are still open, e.g., whether the alloys have a good miscibility so that the mixing cations (Si, Ge, and Sn) can be distributed uniformly in the alloys and how their band gaps depend on alloy composition. To further improve the solar cell performance, these questions need to be addressed. In this paper, we attempt to shine a light on these problems through the first-principles calculation of the structural and electronic properties of the $Cu_2Zn(Sn,Si)Se_4$ and $Cu_2Zn(Sn,Ge)Se_4$ alloys.

II. COMPUTATIONAL DETAILS

The band structure and total energy calculations are performed using the density functional theory based on the generalized gradient approximation (GGA) of Perdew–Burke–Ernzerhof (PBE),[23] as implemented in the Vienna *Ab initio* Simulation Package (VASP) code.[24] The electron and core interactions are included using the frozen-core projector augmented wave (PAW) method,[25] and the plane-wave cutoff energy is chosen as 400 eV in all cases. The 3*d* states of Ge and 4*d* states of Sn are explicitly treated as valence electrons. The Monkhorst-Pack k-point mesh[26] of $4 \times 4 \times 2$ for the 128-atom supercell cell is employed. The lattice vectors and atomic positions for all calculated structures were fully relaxed by minimizing the quantum mechanical stresses and forces.

To accurately calculate the phase diagrams of $Cu_2Zn(Sn,Si)Se_4$ and $Cu_2Zn(Sn,Ge)Se_4$ alloys, semigrand-canonical Monte Carlo simulations are carried out in which the energetics of the alloys are specified by the cluster expansion (CE) Hamiltonian. In this ensemble, the energy and concentration of an alloy with a fixed total number of active atoms (e.g., Sn and Si) are allowed to fluctuate while the temperature and chemical potentials are externally

TABLE I. Atomic coordinates and occupation of the SQS for mixed group-IV cation $Cu_2ZnSn_{1-x}X_xSe_4$ (X = Ge, Si) alloys at concentration $x = 0.25$ and 0.50 used in our calculation. For clarity, only the mixed sublattice coordinates are shown in fractional coordinates.

$Cu_2ZnSn_{1-x}X_xSe_4$			
$x = 0.25$		$x = 0.50$	
Type	Coordinates	Type	Coordinates
Sn	0.250 0.000 0.125; 0.250 0.000 0.625	Sn	0.250 0.000 0.125; 0.250 0.000 0.625
Sn	0.250 0.500 0.125; 0.250 0.500 0.625	Sn	0.750 0.000 0.625; 0.750 0.500 0.625
Sn	0.750 0.000 0.625; 0.750 0.500 0.625	Sn	0.000 0.750 0.375; 0.000 0.250 0.375
Sn	0.000 0.750 0.875; 0.000 0.750 0.375	Sn	0.500 0.750 0.375; 0.500 0.250 0.875
Sn	0.000 0.250 0.875; 0.500 0.750 0.375	X	0.250 0.500 0.125; 0.250 0.500 0.625
Sn	0.500 0.250 0.875; 0.500 0.250 0.375	X	0.750 0.000 0.125; 0.750 0.500 0.125
X	0.750 0.000 0.125; 0.750 0.500 0.125	X	0.000 0.750 0.875; 0.000 0.250 0.875
X	0.000 0.250 0.375; 0.500 0.750 0.875	X	0.500 0.750 0.875; 0.500 0.250 0.375

imposed. The simulation box contains 50×50 unit cells. The phase boundary tracking method[27] is used to determine the average concentration of the alloy. For CE calculations, the effective cluster interactions defining the CE are obtained by a least-square fit to the first-principles calculated total energies of 20 alloys with different Si (or Ge) concentrations;[28] the CE contains point figure and three pair figures.

III. RESULTS OF THE QUARTERNARY COMPOUNDS

A. Mixing enthalpies

The accurate calculation of the properties of semiconductor alloys relies on the accurate description of the randomness of the mixing atoms in the alloys, i.e., the random distribution of Sn and Si at the group-IV sites in $Cu_2Zn(Sn,Si)Se_4$ alloys (Sn and Ge in $Cu_2Zn(Sn,Ge)Se_4$ alloys). In this paper, the special quasirandom structure (SQS) approach[29] is used with a 128-atom (16-mixed Sn/Si and Sn/Ge sites) supercell. In the SQS approach, the mixed Sn/Si or Sn/Ge atoms are arranged in a way such that the atomic correlation function in the mixed group-IV sublattice is closest to that of the random alloys. The atomic site occupations in fractional coordinates for $Cu_2ZnSn_{1-x}X_xSe_4$ (X = Ge, Si) with $x = 0.25$, 0.50, and 0.75 are shown in Table I, and the calculated atomic correlation functions $\bar{\Pi}_{k,m}$ for figures with k vertices and up to the mth neighbor distance are compared with that of the exact random alloys in Table II. As can be seen, the quality of the SQS used in this calculation is reasonable.

TABLE II. Atomic correlation functions $\bar{\Pi}_{k,m}$ of the SQS used in our calculation at concentration $x = 0.25$, 0.5, and compared with the ideal values $(2x-1)^k$ of the random alloy.

	$\bar{\pi}_{2,1}$	$\bar{\pi}_{2,2}$	$\bar{\pi}_{2,3}$	$\bar{\pi}_{2,4}$	$\bar{\pi}_{3,1}$	$\bar{\pi}_{3,2}$	$\bar{\pi}_{4,1}$
	$Cu_2ZnSn_{1-x}X_xSe_4$						
$x = 0.25$							
SQS	1/4	1/4	0	1/4	−1/8	0	0
Random	1/4	1/4	1/4	1/4	−1/8	−1/8	1/16
$x = 0.50$							
SQS	0	0	0	0	0	0	0
Random	0	0	0	0	0	0	0

To describe the miscibility of the alloys, we first calculated the alloy formation enthalpy, which is defined as

$$\Delta H(x) = E(x) - (1-x)E_{Cu_2ZnSnSe_4} - xE_{Cu_2ZnXSe_4}, \quad (1)$$

where $E_{Cu_2ZnSnSe_4}$ and $E_{Cu_2ZnXSe_4}$ are the total energy of pure $Cu_2ZnSnSe_4$ and Cu_2ZnXSe_4 (X = Ge, Si) in the kesterite structure, and $E(x)$ is the total energy of the alloy for composition x. For most conventional alloys the alloy formation enthalpy is nearly a quadratic function of the composition x,[18] i.e.,

$$\Delta H(x) = (1-x)\Delta H(0) + x\Delta H(1) + \Omega x(1-x), \quad (2)$$

where Ω is the interaction parameter, an indicator of the alloy solubility. In Fig. 1(a), the black triangles show the

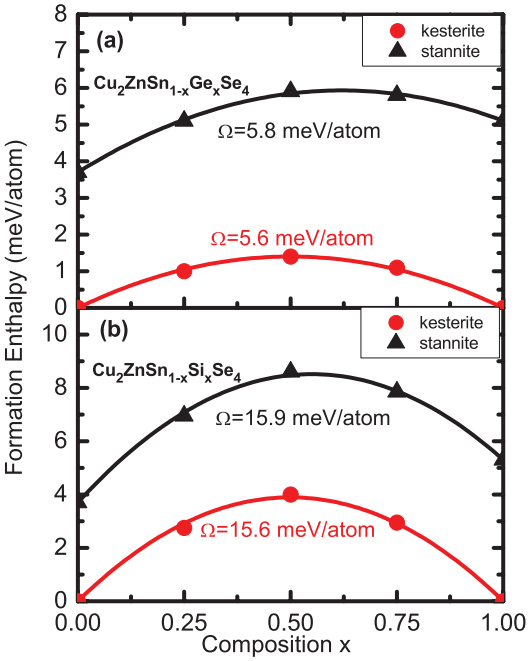

FIG. 1. (Color online) The calculated formation enthalpy for (a) $Cu_2ZnSn_{1-x}Ge_xSe_4$ and (b) $Cu_2ZnSn_{1-x}Si_xSe_4$ alloys as a function of alloy composition x for both kesterite and stannite structures. The fitting curves according to Eq. (2) are also given with the interaction parameters Ω.

calculated formation enthalpy of the kesterite-structured $Cu_2Zn(Sn,Ge)Se_4$ alloys with different composition $x = 0.25$, 0.50, and 0.75. Fitting these data according to Eq. (2) gives the interaction parameter $\Omega = 5.6$ meV/atom (or 44.8 meV/mixed atom) for the kesterite-structured alloys. This value is smaller than that for $Cu_2ZnSn(S_{1-x}Se_x)_4$ ($Cu_2ZnSn(S,Se)_4$) (52 meV/mixed atom)[18] and $Cu(In_xGa_{1-x})Se_2$ (76 meV/mixed-atom),[30] suggesting that component-uniform $Cu_2Zn(Sn,Ge)Se_4$ alloys can be grown easily under the standard growth temperature. Furthermore, in a regular solution model, the miscibility gap temperature is given by Ω(per mixed atom)/2 k_BT. We find that the transition temperature is 260 K for the $Cu_2Zn(Sn,Ge)Se_4$ alloy, confirming that Ge can be easily mixed into $Cu_2ZnSnSe_4$ compounds.

In Fig. 1(b), the calculated formation enthalpy and interaction parameter of $Cu_2Zn(Sn,Si)Se_4$ are also shown. The size and chemical mismatch between Sn and Si is larger than that between Sn and Ge, so the interaction parameter $\Omega = 15.6$ meV/atom (or 124.8 meV/mixed-atom) of the kesterite-structured $Cu_2Zn(Sn,Si)Se_4$ alloys is much larger than the $Cu_2Zn(Sn,Ge)Se_4$ alloys, indicating that Si has smaller solubility in $Cu_2ZnSnSe_4$. In a regular solution model, the transition temperature is 724 K for a $Cu_2Zn(Sn,Si)Se_4$ alloy, much larger than that for $Cu_2Zn(Sn,Ge)Se_4$. Considering, however, that Si is much more earth-abundant and cheaper than Ge and that less Si is needed to tune the band gap to a given value (see below), $Cu_2Zn(Sn,Si)Se_4$ alloys are still competitive with $Cu_2Zn(Sn,Ge)Se_4$ as the photovoltaic materials, despite the smaller solubility.

In order to calculate the miscibility gap temperature accurately, we performed the Monte Carlo simulations based on the CE Hamiltonian. We used three pairs [see Fig. 2(c)] in the CE approach, and the values of effective cluster interactions for the three pairs are −0.003387 (−0.010510), −0.001787(−0.004543), and 0.001791 (0.004343) for $Cu_2Zn(Sn,Ge)Se_4$ ($Cu_2Zn(Sn,Si)Se_4$) alloys. Our calculated temperature-composition phase diagram of $Cu_2Zn(Sn,Ge)Se_4$ and $Cu_2Zn(Sn,Si)Se_4$ alloys were shown in Fig. 2(a) and Fig. 2(b). We can see that the miscibility gap temperature is only 178 K for the $Cu_2Zn(Sn,Ge)Se_4$ alloy and 535 K for the $Cu_2Zn(Sn,Si)Se_4$ alloy from this method. As expected, the regular solution model overestimates the miscibility gap temperatures.

Because $Cu_2ZnSnSe_4$, $Cu_2ZnGeSe_4$, and $Cu_2ZnSiSe_4$ may also adopt the meta-stable stannite structure,[3,31] we have also calculated the formation enthalpies of the $Cu_2Zn(Sn,Ge)Se_4$ and $Cu_2Zn(Sn,Si)Se_4$ alloys in the stannite-based structures. The results are shown in Fig. 1 (black triangles) and referenced to the corresponding values of the kesterite $Cu_2ZnSnSe_4$, $Cu_2ZnGeSe_4$, and $Cu_2ZnSiSe_4$. The interaction parameters of the stannite alloys are similar to that of the kesterite alloy, showing the mixing of the Sn and Ge (Sn and Si) cations is weakly influenced by the specific cation ordering. In addition, the energy differences between kesterite and stannite alloys are kept almost constant (∼5 meV/atom) at different compositions, and the small differences indicate that the kesterite and stannite cation ordering may coexist in the synthesized alloys.

B. Band gap bowing

Since the composition-tunable $Cu_2Zn(Sn,Ge)Se_4$ and $Cu_2Zn(Sn,Si)Se_4$ alloys can be synthesized, we will show how

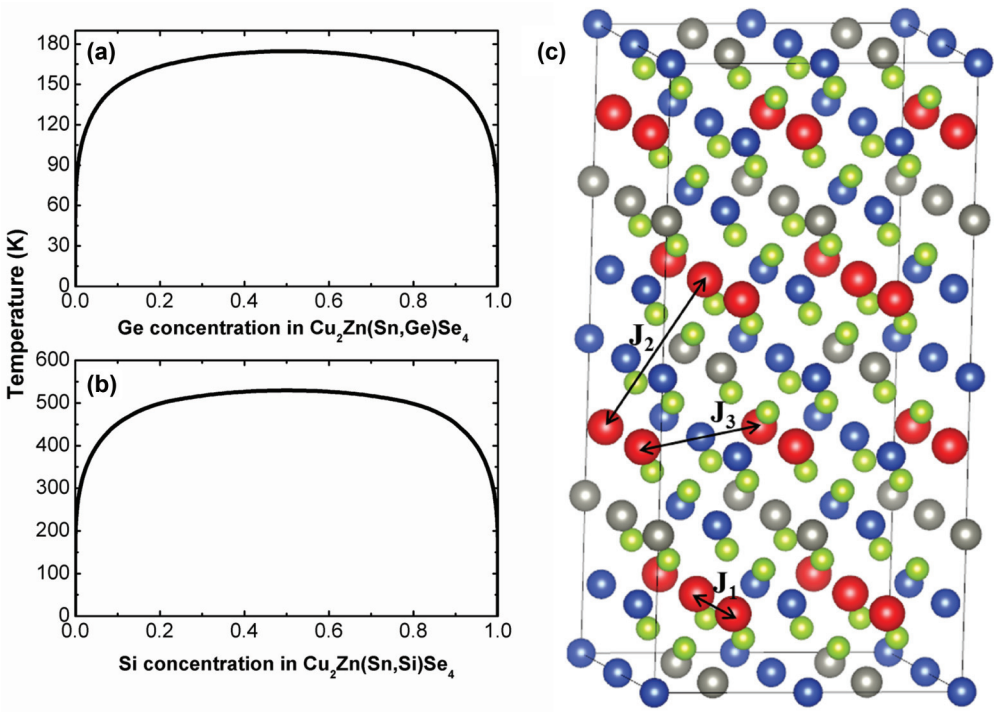

FIG. 2. (Color online) The calculated temperature-composition phase diagram for (a) $Cu_2ZnSn_{1-x}Ge_xSe_4$ and (b) $Cu_2ZnSn_{1-x}Si_xSe_4$ alloys. (c) The three pair interactions (J_1, J_2, and J_3) used in our CE fits. The blue spheres indicate Cu atoms, the gray spheres indicate Zn atoms, the green spheres indicate Se atoms, and the red spheres indicate Sn/Ge atoms in $Cu_2Zn(Sn,Ge)Se_4$ alloys and Sn/Si atoms in $Cu_2Zn(Sn,Si)Se_4$ alloys.

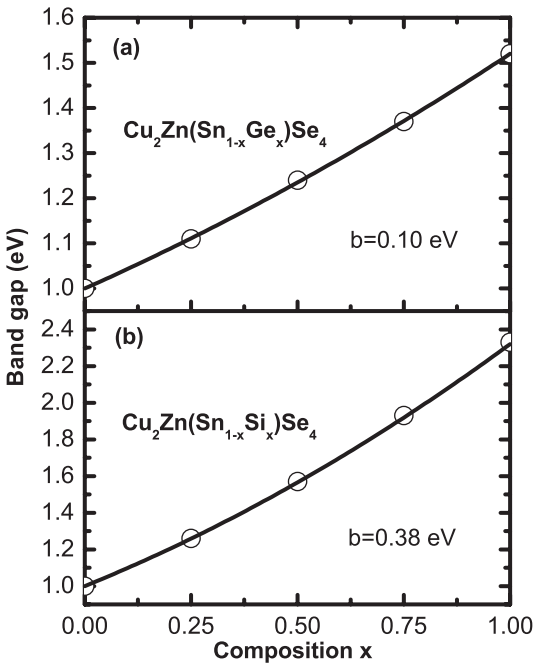

FIG. 3. The band gap of (a) $Cu_2ZnSn_{1-x}Ge_xSe_4$ and (b) $Cu_2ZnSn_{1-x}Si_xSe_4$ alloys as a function of composition x. The band gaps shifted using scissor operator so the band gaps at $x = 0$ and $x = 1$ agree with experimental values.

their band gaps depend on the composition. For random semiconductor alloys, the band gap dependence on the composition can be described by the following equation:

$$E_g(x) = (1-x)E_g(Cu_2ZnSnSe_4) + xE_g(Cu_2ZnXSe_4) - bx(1-x), \quad (3)$$

where E_g is the band gap, and b is the bowing parameter. We calculated the band gaps for $Cu_2Zn(Sn,Ge)Se_4$ and $Cu_2Zn(Sn,Si)Se_4$ alloys with different compositions using the PBE functional and the fitted bowing parameter $b \sim 0.10$ eV for $Cu_2Zn(Sn,Ge)Se_4$ and $b \sim 0.38$ eV for $Cu_2Zn(Sn,Si)Se_4$. It is well known that although the PBE functional underestimates the band gaps, the calculated bowing parameters are accurate because the bowing parameters are derived from the band gap difference so the PBE band gap errors are systematically canceled in the calculation.[18,32] The calculated results are shown in Fig. 3, where a scissor correction is added to the PBE band gaps so that the band gaps at $x = 0$ and $x = 1$ are equal to the experimental values[13,33,34] and the correction is linear with the composition x. In this way, the corrected band gaps at different compositions can be compared directly with the experimental values.

From Fig. 3 we can see that the band gaps of both the $Cu_2Zn(Sn,Ge)Se_4$ and $Cu_2Zn(Sn,Si)Se_4$ alloys increases monotonically and almost linearly with the composition parameter x, consistent with their small bowing parameters. The bowing parameter is slightly larger for $Cu_2Zn(Sn,Si)Se_4$ alloys than $Cu_2Zn(Sn,Ge)Se_4$ alloys, which is easy to understand considering the larger size and chemical differences between Sn and Si (Ref. 30); however, the absolute value is still small, showing the quaternary compounds have good tolerance to the chemical and size difference of the mixed cations. Because the band gap of $Cu_2ZnSiSe_4$ larger than $Cu_2ZnGeSe_4$, the band gap increase with composition is much more significant for $Cu_2Zn(Sn,Si)Se_4$, and only ~40% of Si is needed to alloy into $Cu_2ZnSnSe_4$ to tune the $Cu_2Zn(Sn,Si)Se_4$ band gap to about 1.4 eV. For comparison, about 80% Ge is needed to tune $Cu_2ZnSnSe_4$ to 1.4 eV band gap.

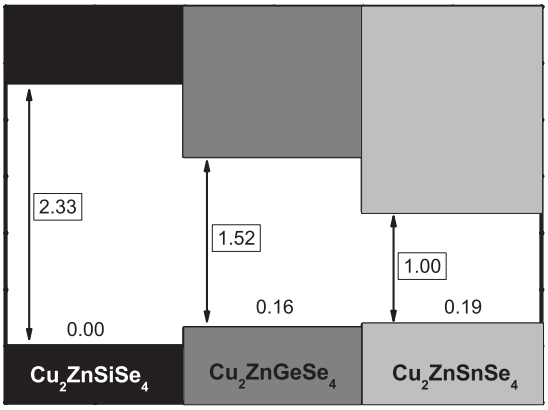

FIG. 4. GGA-calculated valence band alignment between $Cu_2ZnSnSe_4$, $Cu_2ZnGeSe_4$, and $Cu_2ZnSiSe_4$. The experimental band gaps are used to obtain the corresponding conduction band offsets.

C. Band offsets

To understand the band gap increase with the Ge composition in $Cu_2Zn(Sn,Ge)Se_4$ and the Si composition in $Cu_2Zn(Sn,Si)Se_4$, the band offsets for $Cu_2ZnSnSe_4$, $Cu_2ZnGeSe_4$, and $Cu_2ZnSiSe_4$ are calculated using the standard computational approaches.[35,36] As shown in Fig. 4, the valence band maximum (VBM) of the three compounds are close to each other (the offset is less than 0.2 eV), while the conduction band minimum (CBM) shifts up significantly from $Cu_2ZnSnSe_4$, $Cu_2ZnGeSe_4$ to $Cu_2ZnSiSe_4$, with an offset as large as 1.1 eV. The reason for the small valence band offsets is because the VBM of these compounds consists primarily of Se 4p and Cu 3d orbitals;[31,36] therefore, substitution of Sn by Ge or Si does not affect the VBM energies significantly. On the other hand, the CBM is the antibonding state of the hybridization between the group IV (Sn, Ge, Si) s orbitals and Se 4s orbitals. Because Sn-Se bond length is larger than the Ge-Se bond length, the antibonding CBM state of $Cu_2ZnSnSe_4$ has lower energy than that of $Cu_2ZnGeSe_4$, and similarly we can understand the lower CBM energy of $Cu_2ZnGeSe_4$ than $Cu_2ZnSiSe_4$.

According to the calculated band alignment in Fig. 4, the band gap increase of $Cu_2Zn(Sn,Ge)Se_4$ and $Cu_2Zn(Sn,Si)Se_4$ with the Ge and Si composition can be attributed primarily to the conduction band upshift, with a much smaller contribution from the valence band downshift. With a clear understanding on the reason of the band gap increase, we can further predict the electrical conductivity of these alloys. According to the doping limit rule,[37] a material is difficult to be doped n-type if the CBM energy is high and difficult to be doped p-type if the VBM energy is low. Previously, experiments and theoretical calculations have shown that $Cu_2ZnSnSe_4$ samples have intrinsic p-type conductivity and with relatively poor n-type dupability due to the compensation of acceptor defects.

The small valence band offsets shown in Fig. 4 indicates the intrinsic *p*-type conductivity should be expected also in $Cu_2Zn(Sn,Ge)Se_4$ and $Cu_2Zn(Sn,Si)Se_4$ alloys, and the much higher CBM of $Cu_2ZnSiSe_4$ and $Cu_2ZnGeSe_4$ suggests that *n*-type doping could be more difficult in these alloys as the band gap increases.

IV. CONCLUSIONS

In summary, using first-principles calculations, we have investigated the structural and electronic properties of the random alloys $Cu_2ZnSn_{1-x}X_xSe_4$ (X = Ge, Si) as a function of the composition x. We find that the formation enthalpy of $Cu_2Zn(Sn,Ge)Se_4$ is small; therefore, Ge can be easily mixed into $Cu_2ZnSnSe_4$. For $Cu_2Zn(Sn,Si)Se_4$ alloys the formation energy is relatively large but still miscible in a wide range at standard growth temperature. The band gap dependence on the alloy composition is almost linear for both $Cu_2Zn(Sn,Ge)Se_4$ and $Cu_2Zn(Sn,Si)Se_4$ alloys, and the bowing parameter is slightly larger for $Cu_2Zn(Sn,Si)Se_4$ than for $Cu_2Zn(Sn,Ge)Se_4$ due to the larger size and chemical mismatch between Sn and Si. The band gap increase with Si or Ge composition results primarily from the conduction band upshift, and the valence band downshift is small, which indicates these alloys should have intrinsic *p*-type conductivity similar to $Cu_2ZnSnSe_4$ and their *n*-type doping could be difficult. Based on these results, we predict that the band gap-tunable and composition-uniform $Cu_2Zn(Sn,Si)Se_4$ and $Cu_2Zn(Sn,Ge)Se_4$ alloys can be synthesized for photovoltaic application.

ACKNOWLEDGMENTS

The work at Fudan University was partially supported by the Special Funds for Major State Basic Research, National Science Foundation of China (NSFC), International collaboration project of MOST, Pujiang plan, and Program for Professor of Special Appointment (Eastern Scholar). The work at ECNU was supported by NSFC. The work at NREL was funded by the US Department of Energy (DOE) under Contract No. DE-AC36-08GO28308. Computation was performed in the Supercomputer Center of Fudan University.

[1] Q. Guo, H. W. Hillhouse, and R. Agrawal, J. Am. Chem. Soc. **131**, 11672 (2009).
[2] K. Wang, O. Gunawan, T. Todorov, B. Shin, S. J. Chey, N. A. Bojarczuk, D. Mitzi, and S. Guha, Appl. Phys. Lett. **97**, 143508 (2010).
[3] S. Chen, X. G. Gong, A. Walsh, and S.-H. Wei, Appl. Phys. Lett. **94**, 041903 (2009).
[4] C. Perrson, J. Appl. Phys. **107**, 053710 (2010).
[5] A. Nagoya, R. Asahi, R. Wahl, and G. Kresse, Phys. Rev. B **81**, 113202 (2010).
[6] M. León, S. Levcenko, R. Serna, G. Gurieva, A. Nateprov, J. M. Merino, E. J. Friedrich, U. Fillat, S. Schorr, and E. Arushanov, J. Appl. Phys. **108**, 093502 (2010).
[7] H. Matsushita, T. Ochiai, and A. Katsui, J. Cryst. Growth **275**, e995 (2005).
[8] Q. Guo, G. M. Ford, W. C. Yang, B. C. Walker, E. A. Stach, H. W. Hillhouse, and R. Agrawal, J. Am. Chem. Soc. **132**, 17384 (2010).
[9] H. R. Liu, S. Chen, Y. T. Zhai, H. J. Xiang, X. G. Gong, and S.-H. Wei, J. Appl. Phys. **112**, 093717 (2012)
[10] A. Walsh, S. Chen, S.-H. Wei, and X. G. Gong, Adv. Energy Mater. **2**, 400 (2012).
[11] W. Shockley and H. J. Queisser, J. Appl. Phys. **32**, 510 (1961).
[12] I. Repins, C. Beall, N. Vora, C. DeHart, D. Kuciauskas, P. Dippo, B. To, J. Mann, W. C. Hsu, A. Goodrich, and R. Noufi, Solar Energy Materials and Solar Cells **101**, 154(2012).
[13] S. Ahn, S. Jung, J. Gwak, A. Cho, K. Shin, K. Yoon, D. Park, H. Cheong, and J. H. Yun, Appl. Phys. Lett. **97**, 021905 (2010).
[14] T. K. Todorov, J. Tang, S. Bag, O. Gunawan, T. Gokmen, Y. Zhu, D. B. Mitzi, Adv. Energy Mater (2012), doi: 10.1002/aenm.201200348.
[15] W. Ki and H. W. Hillhouse, Adv. Energy Mater. **1**, 732 (2011); K. Timmo, M. Altosaar, J. Raudoja, K. Muska, M. Pilvet, M. Kauk, T. Varema, M. Danilson, O. Volobujeva, and E. Mellikov, Solar Energy Materials and Solar Cells **94**, 1889 (2010); S. Bag, O. Gunawan, T. Gokmen, Y. Zhu, T. K. Todorov, and D. B. Mitzi, Energy Environ. Sci. **5**, 7060 (2012).
[16] S. Chen, J.-H. Yang, X. G. Gong, A. Walsh, and S.-H. Wei, Phys. Rev. B **81**, 245204 (2010).
[17] S. Chen, X. G. Gong, A. Walsh, and S.-H. Wei, Appl. Phys. Lett. **96**, 021902 (2010).
[18] S. Chen, A. Walsh, J.-H. Yang, X. G. Gong, L. Sun, P.-X. Yang, J.-H. Chu, and S.-H. Wei, Phys. Rev. B **83**, 125201 (2011).
[19] S. Chen, L.-W. Wang, A. Walsh, X. G. Gong, and S.-H. Wei, Appl. Phys. Lett. **101**, 223901 (2012).
[20] S. Chen, A. Walsh, X. G. Gong, and S.-H. Wei, Adv. Mater. **25**, 1522 (2013).
[21] G. M. Ford, Q. Guo, R. Agrawal, and H. W. Hillhouse, Chem. Mater. **23**, 2626 (2011).
[22] S. Bag, O. Gunawan, T. Gokmen, Y. Zhu, and D. B. Mitzi, Chem. Mater. **24**, 4588 (2012).
[23] J. P. Perdew, K. Burke, and M. Ernzerhof, Phys. Rev. Lett. **77**, 3865 (1996).
[24] G. Kresse and J. Furthmüller, Phys. Rev. B **54**, 11169 (1996); G. Kresse and J. Furthmüller, Comput. Mater. Sci. **6**, 15 (1996).
[25] G. Kresse and D. Joubert, Phys. Rev. B **59**, 1758 (1999).
[26] H. J. Monkhorst and J. D. Pack, Phys. Rev. B **13**, 5188 (1976).
[27] A. van de Walle and M. Asta, Modelling Simul. Mater. Sci. Eng. **10**, 521 (2002).
[28] A. van de Walle, M. Asta, and G. Ceder, CALPHAD: Comput. Coupling Phase Diagrams Thermochem. **26**, 539 (2002).
[29] S.-H. Wei, L. G. Ferreira, J. E. Bernard, and A. Zunger, Phys. Rev. B **42**, 9622 (1990).
[30] S.-H. Wei and A. Zunger, J. Appl. Phys. **78**, 3846 (1995); Note that in this paper, due to different approaches, the calculated alloy formation energy for $Cu(In_xGa_{1-x})Se_2$ is larger than the one presented in this paper.
[31] S. Chen, X. G. Gong, A. Walsh, and S.-H. Wei, Phys. Rev. B **79**, 165211 (2009).

[32]S.-H. Wei, S. B. Zhang, and A. Zunger, J. Appl. Phys. **87**, 1304 (2000).
[33]C. Lee and C.-D. Kim, J. Korean Phys. Soc. **37**, 364 (2000).
[34]H. Matsushita, T. Ichikawa, and A. Katsui, J. Mater. Sci. **40**, 2003 (2005).
[35]S.-H. Wei and A. Zunger, Appl. Phys. Lett. **72**, 2011 (1998).
[36]S. Chen, X. G. Gong, and S.-H. Wei, Phys. Rev. B **75**, 205209 (2007).
[37]S. B. Zhang, S.-H. Wei, and A. Zunger, J. Appl. Phys. **83**, 3192 (1998).